AUT Journal of Civil Engineering

AUT J. Civil Eng., 9(4) (2025) 337-356
DOI: 10.22060/ajce.2025.24264.5927

The Behavior of High-Strength LC3 Concrete Reinforced with Recycled Steel Fiber under Uniaxial Compression and Splitting Tensile

Saeed Sedighi, Alireza Rahai, Faramarz Moodi*

Department of Civil and Environmental Engineering, Amirkabir University of Technology, Tehran, Iran.

ABSTRACT: This study assesses the stress-strain and load-deflection behavior of ordinary Portland cement (OPC) and limestone low kaolinite calcined clay cement (LC3) concrete under uniaxial compressive and indirect splitting loads. For this, ten concrete mixes were designed, half of which were LC3-based concrete. In the LC3-based concrete, 30% of cement was substituted with the limestone and calcined clay mixture. Four different contents of recycled tire steel fiber (RTSF) were used for reinforcing the concrete. The uniaxial compression and indirect splitting tensile tests were performed on the cylinder specimens. Peak strain, ultimate strain, absorbed energy, and toughness in compression were evaluated to assess the uniaxial compression behavior of plain and RTSF-reinforced OPC and LC3-based concrete. Also, absorbed energy and toughness in splitting were determined to examine the splitting behavior. The results demonstrated that at least 0.6% RTSF is required to develop the post-peak phase of the stress-strain curve under uniaxial compression. Further, the LC3 concrete resulted in lower peak and ultimate strains under compressive load. Incorporating 1.2% RTSF into OPC concrete enhanced the peak and ultimate strains by about 20% and 94%, respectively. In addition, the inclusion of 0.9% RTSF in LC3 concrete improved the peak and ultimate strains by approximately 18% and 100%, respectively. Furthermore, the LC3 concrete demonstrated better performance in the post-peak phase of splitting tensile. Moreover, digital image correlation (DIC) results demonstrated that incorporating RTSF into concrete effectively controls the initiation and propagation of cracks.

Review History:
Received: Jun. 09, 2025
Revised: Nov. 30, 2025
Accepted: Dec. 05, 2025
Available Online: Dec. 09, 2025

Keywords:
FRC-LC3
Mechanical Properties
Energy Absorption
Toughness
DIC

1- Introduction

Concrete is the most used construction material in civil projects such as bridges, port structures, and transportation infrastructures [1-3]. Choosing sustainable materials is essential for reducing the carbon footprint of construction projects [4]. Limestone-Calcined Clay-Cement (LC3) concrete is an encouraging alternative to ordinary concrete due to many benefits, such as extensive resources of suitable clays worldwide [5, 6], higher strength in the long term [7, 8], lower bleeding [7-9], finer pore structures [10], lesser permeability [10, 11], and better durability in a chloride environment [12]. Also, Pillai et al. [13] reported that LC3 concrete with similar strength to OPC concrete leads to remarkably lower CO_2 emission. The investigation by Zolfagharnasab [14] showed that partial cement replacement by low kaolinite calcined clay could yield compressive strength comparable to that of ordinary cement concrete. However, with the synergic interaction of the low kaolinite calcined clay and limestone in LC3 concrete, better compressive strength can be obtained compared to using only calcined clay. The consumption of calcium carbonate hydroxide by the synergic interaction of limestone and calcined clay was stated as the reason for the better performance of the LC3 concrete [15]. Argın et al. showed that limestone enhanced the pozzolanic reactivity of the calcined clay by producing carboaluminate phases and providing a nucleation effect [16].

The brittle nature and low tensile strength of concrete lead to a lack of resistance against crack propagation. One of the solutions to overcome this weakness is adding fibers to concrete as a reinforcing material [17-19]. Steel fibers positively affect the mechanical properties of the brittle nature of plain concrete, such as hindering crack formation and propagation, increasing the tensile and residual strength, and significantly enhancing the energy absorbed and toughness [20, 21]. Aiello et al. [22] reported that including 0.26% of recycled tire steel fibers (RTSF) in concrete leads to a 12% enhancement in compressive strength. A study by Hu et al. [23] revealed that incorporating about 0.38% RTSF increments the compressive strength by about 10%. Krolo et al. [24] proved that a low amount of recycled steel fibers had an insignificant effect on the compressive strength. Another study revealed that adding recycled steel fibers up to a threshold of 0.5% caused an enhancement of about 5% in compressive strength, while utilizing more fibers (0.75%) led to a drop of 8% in compressive strength. The reduction in compressive strength was attributed to the poor distribution

*Corresponding author's email: fmoodi@aut.ac.ir

of RTSF and non-homogeneity in the paste matrix due to incorporating high dosages of fibers [25]. Besaci et al. [26] investigated the effect of RTSF on the mechanical properties of concrete by incorporating 0.5, 0.8, 1, and 1.5% RTSF. Their results showed the compressive strength reduced by about 10% when 1.5% RTSF was added. Similarly, adding 0.46% of recycled steel fibers resulted in a slight decrease in compressive strength. It was indicated that the random distribution of RTSF may form fiber bundles that contribute to discontinuities in the paste matrix [27]. In addition, the shape, surface morphology, and rubber particles on the fiber surface can influence the compressive strength and performance of RTSF in concrete. The hydrophobic nature of attached rubber particles can weaken the bonding between RTSF and the paste matrix, negatively impacting compressive strength [26, 28]. However, it has been demonstrated that using recycled steel fibers can enhance the ductility at failure and extend the collapse time of concrete [29]. Furthermore, studies mentioned that incorporating 0.6% and 0.75% RTSF into plain concrete enhanced the splitting strength by about 14% and 28%, respectively [30, 31]. Farhan et al. [32] claimed that recycled steel fibers with different diameters and lengths could provide additional interlocking, which led to a 50% enhancement in splitting strength by including 0.75% RTSF in pavement. Analogously, other experiments revealed that adding recycled steel fibers to the concrete could improve the splitting strength compared to plain concrete. The increase in splitting strength was assigned to arresting the cracks by RTSF after the development of internal cracks in concrete [9, 33, 34]. On the other hand, utilizing inadequate RTSF in the concrete caused a decrease in splitting strength by producing irregularities in the paste matrix [31]. For example, adding RTSF up to 0.375% caused a reduction of splitting strength by about 20% compared to plain concrete [35]. Similarly, a study by Leone showed that adding 0.46% RTSF to the concrete caused a slight decrease in splitting strength [27].

Despite extended research on the mechanical properties of OPC-based concrete reinforced with RTSF, there are no detailed studies on the stress-strain behavior under uniaxial compression. Similarly, the load-displacement behavior of concrete reinforced with RTSF under indirect splitting tensile needs to be clarified. Doubtless, the splitting failure mode of concrete with different amounts of RTSF needs a more detailed study. Further, the effect of the combined use of LC3 and RTSF in concrete should be assessed to investigate the feasibility of employing LC3 as an alternative to OPC concrete in the construction industry.

This study aims to examine the stress-strain and load-deflection behavior of fibrous OPC and LC3 concrete under uniaxial compressive and indirect splitting loads, respectively. The main idea of this research is to combine the RTSF and LC3 to provide green fiber-reinforced concrete in the construction industry. In addition, this study tries to find the minimum required RTSF that develops the post-peak phase under uniaxial compression and indirect splitting. For investigating the effects of RTSF, volume fractions of 0.3, 0.6, 0.9, and 1.2% were incorporated into OPC and LC3-based concrete. The peak and ultimate strains of concrete were examined under uniaxial compression. Furthermore, the absorbed energy and toughness were calculated in uniaxial compression and indirect splitting tensile to evaluate the ductility. Finally, the digital image correlation technique was employed to find the failure mode of recycled fiber-reinforced concrete under indirect splitting tensile. The results of this research can be used for finite element modeling of the structural elements.

2- Materials and Mix Proportion

2- 1- Materials

Natural river sand and crushed gravel were used as aggregates in this study. The aggregates were graded according to ASTM C33 [36], and the results are presented in Table 1. The water absorption and relative density of the sand were recorded as 3.19% and 2.52, respectively, by following ASTM C128 [37]. Similarly, according to ASTM C127 [38] The water absorption and relative density of gravel were determined to be 2.09% and 2.57, respectively. The river sand and crushed gravel were combined with a ratio of 60% and 40% of the total aggregate in the concrete mix, respectively. Three binders were utilized, such as ordinary Portland cement type II, low-kaolinite calcined clay, and limestone powder finer than 75 μm. The results of the chemical compositions of binders are presented in Table 2, which were gained by X-ray Fluorescence (XRF). Additionally, the density of the binders is listed in Table 2. The calcination of raw clay (with about 31% kaolinite) was performed by the electrical furnace according to the procedure mentioned in the previous study [14]. Then, the calcined clay was placed in the ball mill to achieve the desired fineness. Recycled steel fibers from unused tires were employed to reinforce the concrete. The recycled steel fibers have different lengths and geometries. Further, more than 75% of fibers have a length between 10 and 40 mm. Also, the mechanical properties of the RTSF are depicted in Table 3.

2- 2- Mix Proportion

Ten mixes were considered to investigate the behavior of OPC and LC3 concrete reinforced with steel fibers extracted from waste tires under uniaxial compression and indirect splitting tensile: four fibrous OPC concrete, four fibrous LC3 concrete, plain OPC concrete, and plain LC3 concrete. Based on the literature, using about 0.3% RTSF leads to the development of compressive and splitting strength. Also, adding more 1% RTSF in concrete increases the risk of fiber bundling and the demand for superplasticizer, which negatively impacts the fresh and hardened properties of the concrete. Thus, the maximum fiber dosage was chosen to be 1.2%. In OPC and LC3-based concrete, RTSF was included with the volume fractions of 0.3%, 0.6%, 0.9%, and 1.2% as reinforcing materials. The w/b was considered 0.4 for all ten mixes. To produce LC3-based concrete, 30% of cement was replaced by a mixture of low kaolinite calcined clay and

Table 1. The grading of the aggregates used in this study.

	sieve size (mm)											
	37.5	25	19	12.5	9.5	4.75	2.38	1.19	0.6	0.3	0.15	0.075
river sand	100	100	100	100	100	98	74	50	38	23	9	1
crushed gravel	100	100	100	99	77	10	2	0	0	0	0	0
the combination	100	100	100	100	91	63	45	30	23	14	5	0.6

Table 2. Chemical composition and density of binders utilized in this study.

Binders	CaO (%)	SiO_2 (%)	Al_2O_3 (%)	Fe_2O_3 (%)	MgO (%)	P_2O_5 (%)	TiO_2 (%)	SO_3 (%)	Na_2O (%)	K_2O (%)	L.O.I (%)	density (gr/cm^3)
Limestone	55	0.9	0	0.1	0.41	0.03	0	0.25	0	0	43.1	2.71
Calcined clay	6	73	12.7	0.75	0.24	0.11	0.06	0	0.08	0.3	6.18	2.69
Cement	66	18	2.02	4.64	1.11	0.06	0.23	4.6	0.37	1	1.04	3.15

Table 3. The physical properties of RTSF used in this study.

length	diameter	tensile strength	specified gravity	elastic modulus
mm	mm	MPa	gr/cm^3	GPa
0-70	0.18-0.22	3128	7.85	210

limestone powder. The calcined clay and limestone powder were incorporated with a 2:1 ratio in the concrete [6, 10, 14]. The details of all ten mixes are listed in Table 4. A pan mixer was employed to mix the materials. The slump test was performed on the fresh concrete according to ASTM C143 [39]. The target slump for fresh concrete was 13 to 15 cm. For this, different amounts of superplasticizer were added to fresh concrete to keep the slump fixed. As can be seen in Table 4, the demand for superplasticizer was enhanced by incorporating further RTSF into concrete. Namely, including 1.2% RTSF in OPC concrete increased the demand for SP by about 2 times. Previous studies [22, 40] stated that using RTSF in concrete negatively impacts the workability of concrete. In addition, inconsistency in the shape, size, and geometry of RTSF leads to the balling effect in the fresh concrete. One of the solutions is to increase the SP in the fresh concrete to enhance the workability [41, 42]. Also, LC3-based concrete required more superplasticizers compared to similar OPC-based concrete, which agrees with the previous study [43]. It should be noted that the simultaneous use of RTSF and LC3 contributes to extremely high demand for SP. For example, LC3 concrete with 1.2% RTSF required more than 2 times SP compared to plain OPC concrete.

3- Test method

3- 1- Uniaxial Compression

Fig. 1a represents the uniaxial compression setup for recording the compressive strength and stress-strain curve of concrete. The compressive strength test was followed by ASTM C39/C39M [44]. The test was conducted on 100x200 mm cylinders after 28 days of curing in saturated lime water. To ensure uniform compressive stress was applied to the specimens, the sections were capped with sulfur mortar. The test was performed by a 1000 kN servo-electric SANTAM device with a vertical displacement rate of 1.2 mm/min. As shown in Fig. 1a, the test setup includes a fixture with three LVDTs. These LVDTs record the mid-height vertical displacement of the specimen. Three LVDTs recorded the uniaxial displacement of the specimens during the test. Three specimens were considered to be tested for each concrete mix, and the average values were reported.

3- 2- Indirect Splitting Tensile

The indirect splitting tensile test was performed by a DARTEC hydraulic machine according to ASTM C496/C496M [45]. The rate of the vertical displacement was set at 1.2 mm/min. The test fixture is demonstrated in Fig. 1b. The

Table 4. The mixed proportion of different concrete systems investigated in this study.

Mix code	Cement Kg/m^3	limestone Kg/m^3	calcined clay Kg/m^3	Water Kg/m^3	Fiber Kg/m^3(%)	Sand Kg/m^3	Gravel Kg/m^3	SP Kg/m^3
OPC	450	0	0	180	0.0(0%)	1002	680	2.25
OPC-0.3*	450	0	0	180	23.6(0.3%)	997	677	2.5
OPC-0.6	450	0	0	180	47.1(0.6%)	993	674	2.9
OPC-0.9	450	0	0	180	70.7(0.9%)	988	671	3.4
OPC-1.2	450	0	0	180	94.2(1.2%)	984	668	4
LC3	315	45	90	180	0.0(0%)	989	672	3.25
LC3-0.3**	315	45	90	180	23.6(0.3%)	983	667	3.5
LC3-0.6	315	45	90	180	47.1(0.6%)	980	665	3.9
LC3-0.9	315	45	90	180	70.7(0.9%)	976	662	4.4
LC3-1.2	315	45	90	180	94.2(1.2%)	971	659	5

*: OPC-based concrete reinforced with 0.3% recycled steel fiber
**: LC3-based concrete reinforced with 0.3% recycled steel fiber

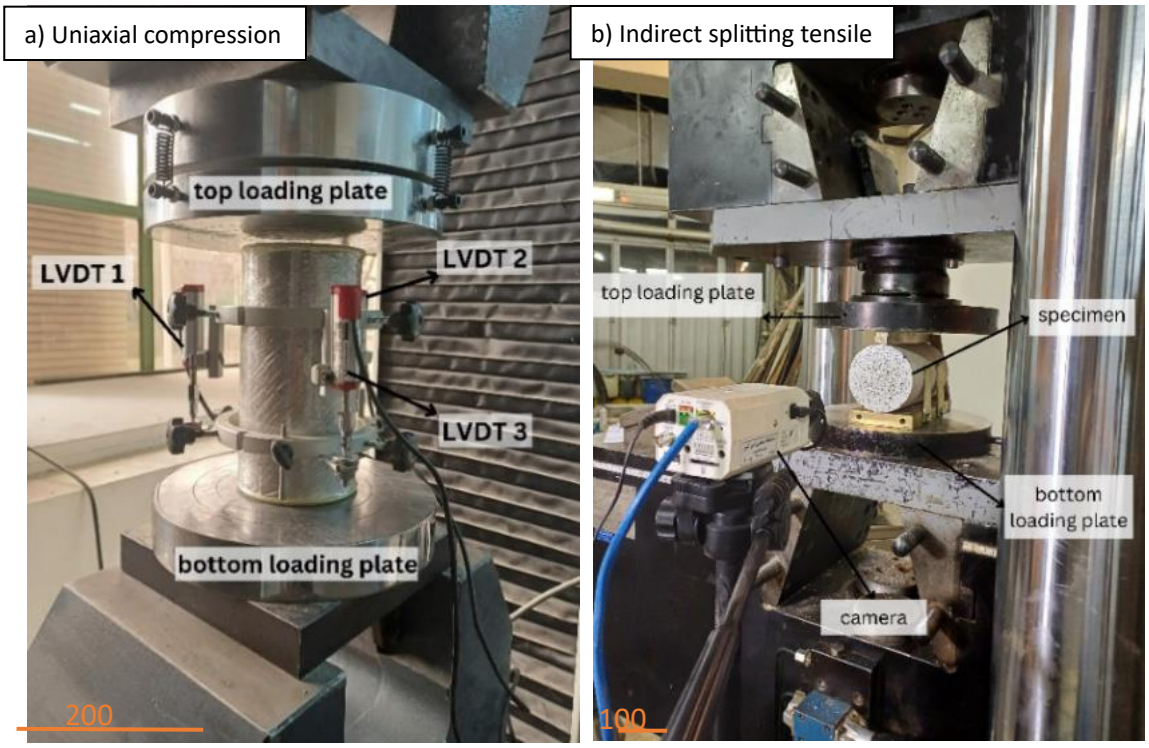

Fig. 1. Test setup for a) uniaxial compression test, b) indirect splitting tensile test.

100x200 mm (diameter x height) cylinders were considered for evaluation of splitting strength. Three specimens were considered for each concrete mix, and the average values were reported. Also, the equipment for digital image processing, including lighting and a high-resolution camera, is presented in Fig. 1b.

4- Results and Discussion

4- 1- Uniaxial Compression

4- 1- 1- Stress-Strain Response

Table 5shows that compressive strength was more than 50 MPa for all concrete systems, categorizing them as high-strength concrete. Adding RTSF with different volume fractions to the OPC and LC3 concrete caused a slight change in the compressive strength. As can be seen in Table 5, the compressive strength of OPC and LC3-based concrete was enhanced by adding RTSF up to 0.3% and 0.9%, respectively. However, the compressive strength dropped when incorporating more than the mentioned amounts of RTFS into the OPC and LC3 concrete. As stated in previous studies, bridging and arresting the cracks with fibers enhances compressive strength [23, 46]. At the same time, a survey by Aghaee et al. [25] revealed that utilizing more than 0.5% RTSF decreases the homogeneity of the paste matrix, which leads to a drop in compressive strength. Similarly, the maximum compressive strength was obtained when 0.4% RTSF was included in concrete [47]. As a result, the non-homogeneity and discontinuity in the paste matrix due to incorporating more than 0.3% and 0.9% RTSF into OPC and LC3 concrete, respectively, overcomes the bridging action of RTSF and drops the compressive strength. Except for LC3-based concrete reinforced with 1.2% RTSF, other LC3-based concrete showed lesser compressive strength compared to OPC-based concrete with a similar amount of RTSF. The coefficient of variation (COV) demonstrates the variability of the results of tested specimens for each concrete mix. It was stated in a previous study [48] that the COV is categorized as excellent, very good, good, fair, and poor when the COV values are less than 2%, 2-3%, 3-4%, 4-5%, and more than 5%, respectively. According to the calculated amounts for COV in Table 5, it is guaranteed that the test results are acceptable.

Although the compressive strength of the concrete is the most important mechanical property for design purposes, the compressive stress-strain curve of concrete under uniaxial compression is crucial for designing concrete structures, numerical analysis, and theoretical analysis. In addition, the safe design of concrete elements requires the deformation and bearing capacity of concrete, which can be determined using the compressive stress-strain curve. The stress-strain curve of non-reinforced and RTSF-reinforced OPC and LC3-based concrete under uniaxial compression is demonstrated in Figs. 2 and 3, respectively. There is no evident change in the post-peak phase of OPC concrete reinforced by 0.3% RTSF compared to non-reinforced OPC-based concrete. In contrast, adding 0.6% and 0.9% RTSF developed the post-peak phase of the compressive stress-strain curve. Interestingly, adding 1.2% RTSF significantly affected the post-peak phase of OPC-based concrete. Among LC3-based concrete reinforced with different amounts of RTSF, adding 0.3% RTSF did not develop the post-peak phase of the stress-strain curve. However, reinforcing LC3-based concrete with 0.6% RTSF developed the post-peak phase as the softening part of the stress-strain curve. The LC3-0.9 and LC3-1.2 experienced very ductile behavior under uniaxial compression. Differently, LC3-based concrete reinforced with 0.9% RTSF showed extreme ductility and energy absorption after peak stress. The microfibers control the micro-cracks at the early ages of the loading, and by increasing the load, the microfibers restrain the macro-cracks [49]. Using the hybrid length of the fibers can restrain and bridge the multi-scale cracks in the cementitious composites [50]. During the extraction of RTSF, steel fibers with varying lengths are generated. Adding recycled steel fibers from expired tires with short and long lengths develops a hybrid steel fiber reinforced concrete. It can control the multi-stage cracks and improve the descending phase of the compressive stress-strain curve. The hybrid action of RTSF in both OPC and LC3-based concrete was effective when a volume fraction of at least 0.6% was used. Regardless of the binder system, adding more than 0.9% RTSF to the concrete led to remarkable ductile failure when the uniaxial compressive load was applied.

Table 5. The compressive strength of OPC and LC3-based concrete.

Mix code	OPC	OPC-0.3	OPC-0.6	OPC-0.9	OPC-1.2
$f'_c\ (MPa)$	55.8	59.42	59.34	57.86	53.18
COV (%)	2.07	1.44	4.55	2.58	1.69
Mix code	LC3	LC3-0.3	LC3-0.6	LC3-0.9	LC3-1.2
$f'_c\ (MPa)$	52.5	53.57	54.28	56.07	54.11
COV (%)	1.57	1.86	0.12	2.06	2.91

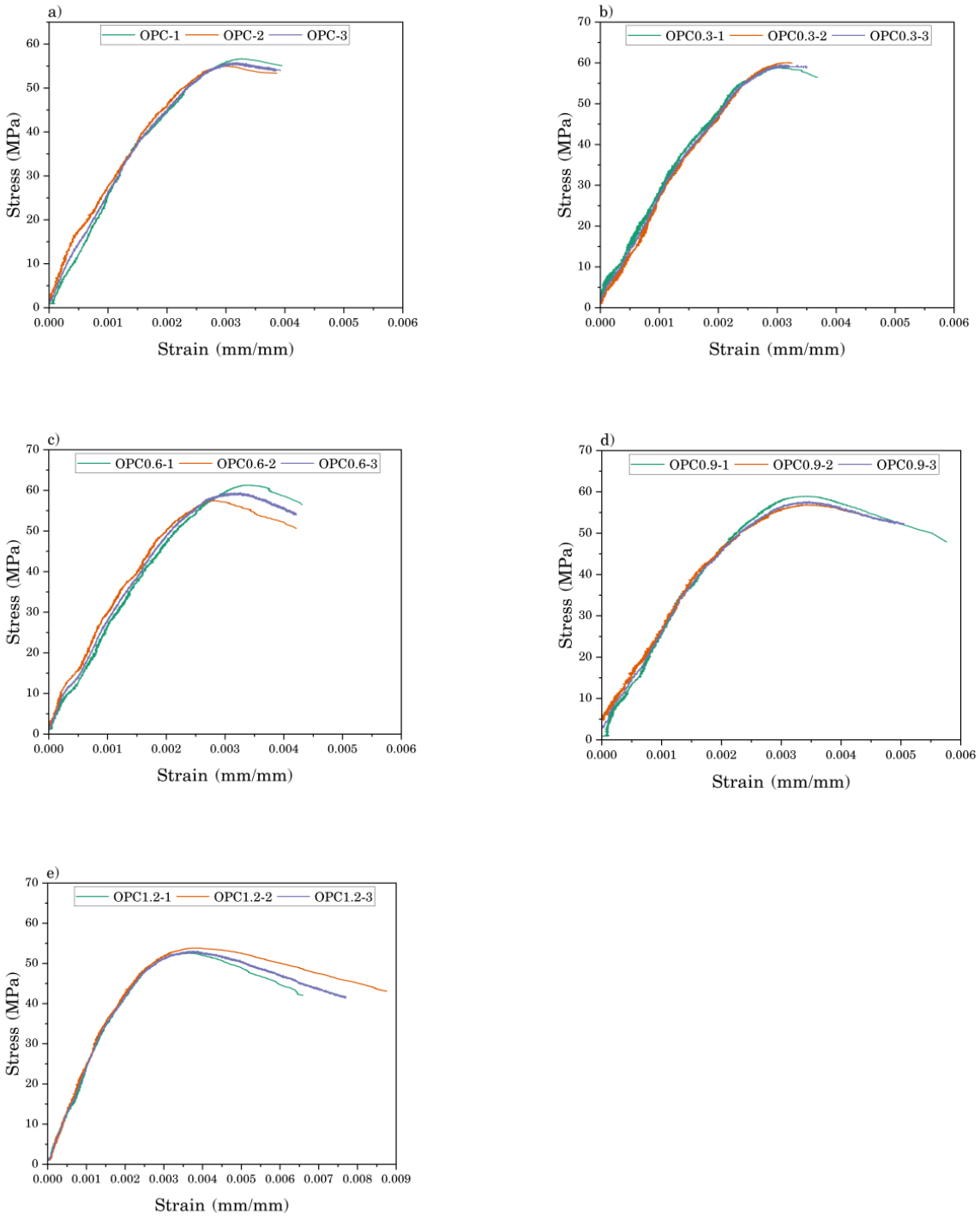

Fig. 2. The stress-strain curves of OPC concrete under uniaxial compressive load.

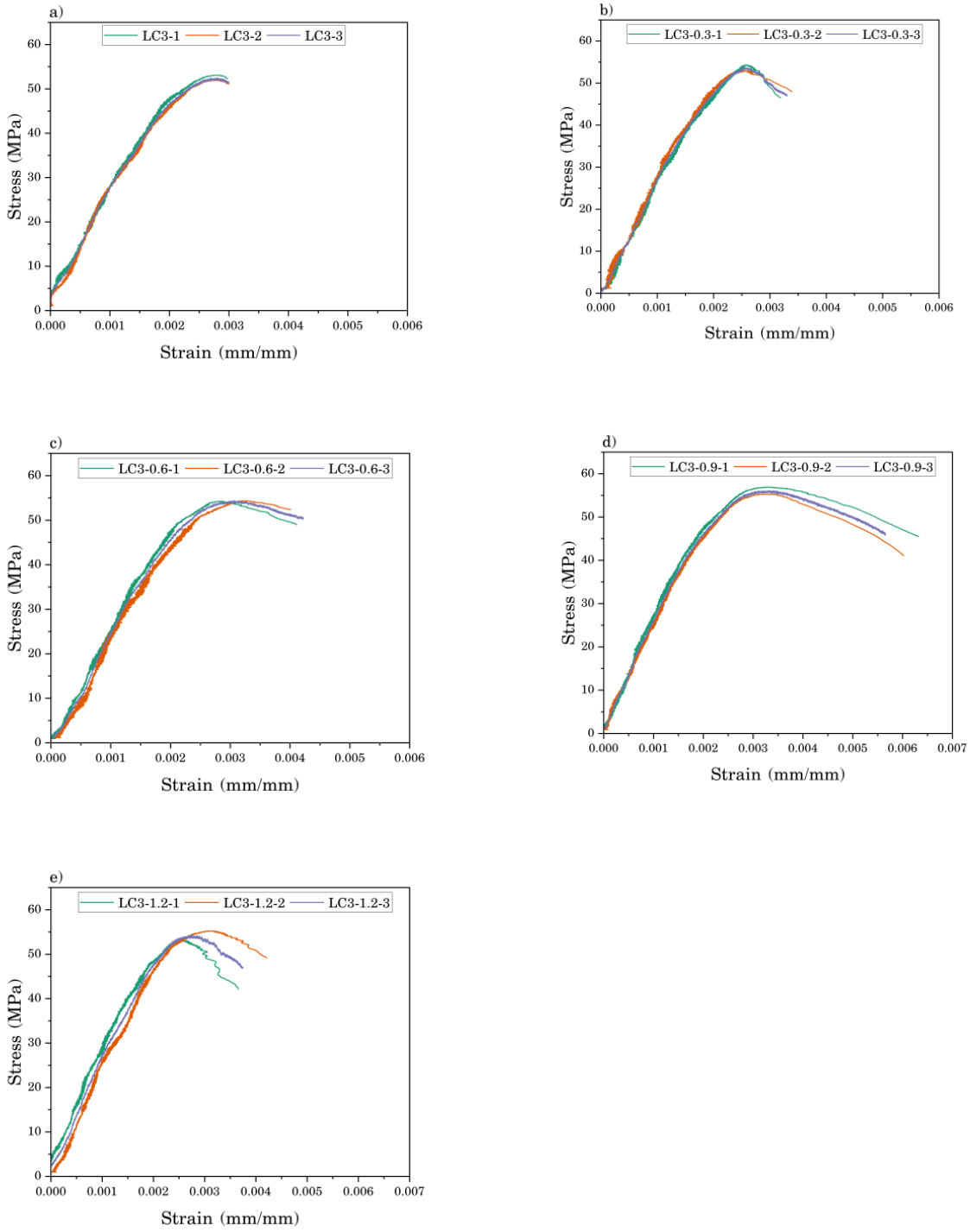

Fig. 3. The stress-strain curves of LC3 concrete under uniaxial compression.

4- 1- 2- Peak Strain (ε_p) and Ultimate Strain (ε_{cu})

Peak and ultimate strains are two essential parameters of the stress-strain curve that describe the behavior of concrete under uniaxial compression. The peak strain corresponds to the peak strength of the compressive stress-strain curve. The concrete's ultimate strain is used to design the structural elements [51, 52]. In addition, the ultimate strain of concrete is used to determine the allowable degree of failure of the concrete [53]. The ultimate strain of the conventional concrete is assumed to be 0.003 in the ACI code for designing concrete elements [54]. In this study, 30 percent of cement was substituted with the low kaolinite calcined clay and limestone. Moreover, various volume fractions of RTSF were incorporated into concrete as a reinforcing material. These two additives can affect the peak and ultimate strains of the concrete when exposed to uniaxial compression. Fig. 4a depicts the peak strain of non-reinforced and reinforced concrete for OPC and LC3-based concrete under uniaxial compressive load. In the OPC-based concrete, the peak strain was recorded at 0.00313 for non-reinforced concrete. Additionally, the peak strain reached a minimum amount of 0.00310 at 0.6% RTSF-reinforcement, then increased sharply to 0.00341 and 0.00377 when the RTSF content rose to 0.9 and 1.2%, respectively. The peak strain of LC3-based concrete without reinforcement was obtained at about 0.0028. The minimum amount of 0.00256 for peak strain occurred at 0.3% RTSF and reached the maximum of 0.0033 in the LC3-0.9. Interestingly, LC3-1.2 resulted in a peak strain of 0.00281, which was lower compared to LC3-0.9. The high-strength concrete without fibers exhibits brittle post-peak behavior. As a result, the specimen collapses suddenly at the ultimate strain under a uniaxial compressive load. The ultimate strain is defined as the strain corresponding to the stress of 80% of the peak stress in the post-peak phase of the stress-strain curve [55]. For high-strength specimens that fail at a stress higher than 80% of peak stress, the ultimate strain is defined as the strain corresponding to the collapse stress. Fig. 4b represents the ultimate strain of non-reinforced and fiber-reinforced concrete for the OPC and LC3-based concrete. The ultimate strain recorded was about 0.00391 for non-reinforced OPC-based concrete. By adding 0.3% RTSF, the ultimate strain dropped to 0.00344, while reinforcing with 0.6%, 0.9%, and 1.2% RTSF increased the ultimate strain to 0.00426, 0.00505, and 0.00767. In contrast, the LC3-based concrete did not follow this trend. The ultimate strain was recorded at about 0.3% for non-reinforced LC3 concrete and then increased to 0.00599 by incorporating 0.9% RTSF into the LC3-based concrete. The ultimate strain decreased to 0.00422 in the 1.2% reinforced LC3 concrete. It was stated by G.M. Ren et al. [56] that the steel fibers restrict the lateral expansion of the specimen under axial compression, allowing it to undergo more axial deformation. Similarly, incorporating RTSF into concrete caused further ultimate strain than plain OPC and LC3 concrete. The LC3-based concrete exhibited a lower peak strain than the OPC-based concrete with similar RTSF content. Additionally, all LC3-based concretes, except LC3-0.9, showed a lower amount of ultimate strain compared to OPC-based concrete under uniaxial compression. The consumption of calcium hydroxide by low-kaolinite calcined clay contributes to denser C-S-H gel, as reported by Chen et al. [57]. The denser microstructure makes the LC3 concrete more brittle than OPC concrete under uniaxial compression, which can be reflected in lower peak and ultimate strains.

Polynomial relations were developed using nonlinear regression for the peak and ultimate strains of OPC and LC3-based concrete reinforced with varying amounts of RTSF. The results of the developed relations are presented in Table 6. According to the developed relations, OPC-based concrete reinforced with RTSF exhibited strong relations for peak and ultimate strains under uniaxial compression with

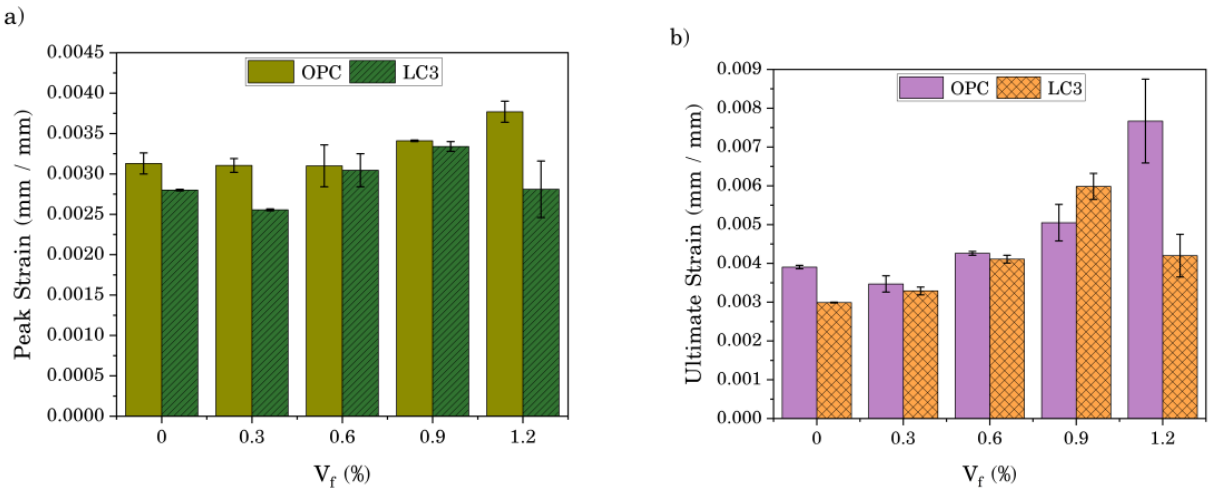

Fig. 4. a) peak strains, b) ultimate strains under uniaxial compression.

Table 6. The developed relations for peak and ultimate strains of concrete containing different amounts of RTSF.

Variables	Developed relations
ε_p vs v_f for OPC	$\varepsilon_{(p,rsf)_{OPC}} = \mathrm{C} + \mathrm{B} * v_f + \mathrm{A} * {v_f}^2$ Eq. (1) $C = 0.00314 \pm 2.79 * 10^{-5}$ $LCL = 0.00302$ and $UCL = 0.00326$ $B = -3.6880 * 10^{-4} \pm 1.0269 * 10^{-4}$ $LCL = -8.1064 * 10^{-4}$ and $UCL = 7.3040 * 10^{-5}$ $A = 7.4508 * 10^{-4} \pm 8.9432 * 10^{-5}$ $LCL = 3.6028 * 10^{-4}$ and $UCL = 0.00113$ $residual\ sum\ of\ square = 0.126$, $R^2\ (COD) = 0.99$, $Adj.R\ square = 0.99$
ε_p vs v_f for LC3	$\varepsilon_{(p,rsf)_{LC3}} = \mathrm{C} + \mathrm{B} * v_f + \mathrm{A} * {v_f}^2$ Eq. (2) $C = 0.0028 \pm 1.5021 * 10^{-5}$ $LCL = 0.00261$ and $UCL = 0.00299$ $B = -0.00152 \pm 1.2284 * 10^{-4}$ $LCL = -0.00308$ and $UCL = 3.7241 * 10^{-5}$ $A = 0.00237 \pm 2.0224 * 10^{-4}$ $LCL = -1.9912 * 10^{-4}$ and $UCL = 0.00494$ $residual\ sum\ of\ square = 2.25$, $R^2\ (COD) = 0.99$, $Adj.R\ square = 0.98$
ε_{ult} vs v_f for OPC	$\varepsilon_{(ult,rsf)_{OPC}} = \mathrm{C} + \mathrm{B} * v_f + \mathrm{A} * {v_f}^2$ Eq. (3) $C = 0.0039 \pm 4.8870 * 10^{-5}$ $LCL = 0.00369$ and $UCL = 0.00411$ $B = -0.00187 \pm 7.0228 * 10^{-4}$ $LCL = -0.00489$ and $UCL = 0.00115$ $A = 0.00408 \pm 0.00112$ $LCL = -7.6002 * 10^{-4}$ and $UCL = 0.00981$ $residual\ sum\ of\ square = 2.3699$, $R^2(COD) = 0.95$, $Adj.R\ square = 0.91$
ε_{ult} vs v_f for LC3	$\varepsilon_{(ult,rsf)_{LC3}} = \mathrm{C} + \mathrm{B} * v_f + \mathrm{A} * {v_f}^2$ Eq. (4) $C = 0.00299 \pm 9.8934 * 10^{-6}$ $LCL = 0.00286$ and $UCL = 0.00312$ $B = -3.2512 * 10^{-4} \pm 5.0462 * 10^{-4}$ $LCL = -0.00674$ and $UCL = 0.00609$ $A = 0.0038 \pm 8.2146 * 10^{-4}$ $LCL = -0.00663$ and $UCL = 0.01424$ $residual\ sum\ of\ square = 0.98$, $R^2(COD) = 0.99$, $Adj.R\ square = 0.98$

ε_p : peak strain (mm/mm), ε_{ult}: ultimate strain (mm/mm), v_f: fiber volume fraction (%)

an R^2 and Adj. R^2 values exceeding 0.95. By neglecting the peak and ultimate strains of LC3-1.2, the strong relations were achieved for LC3-based concrete, with R^2 and Adj. R^2 values exceeding 0.98. Notably, the peak and ultimate strains of LC3-based concrete reinforced with RTSF decreased when the fiber volume increased from 0.9 to 1.2, negatively impacting the developed relations.

4- 1- 3- Absorbed Energy and Toughness Index

Pre-peak energy absorbed in compression () is taken as the area under the stress-strain curve from zero to peak stress [58, 59]. The pre-peak energy absorbed in the compression of RTSF-reinforced concrete is shown in Fig. 5a. The OPC-based concrete reinforced with 0.3% and 0.6% RTSF showed a slight increase in pre-peak energy absorption compared to plain OPC-based concrete. Adding 0.9 and 1.2% RTSF to the plain OPC-based concrete increased pre-peak absorbed energy by about 16% and 23%, respectively, compared to non-reinforced OPC concrete. Adding 0.3% RTSF to the LC3-based concrete decreased the pre-peak energy by about 14%, while adding 0.6% and 0.9% RTSF increased the pre-crack energy by about 8% and 36%, respectively. Interestingly, LC3-1.2 resulted in the same pre-peak energy absorption as non-reinforced LC3 concrete. The highest value of pre-peak energy absorption was calculated for LC3-0.9. Generally, all LC3-based concrete reinforced with RTSF exhibited less pre-peak absorbed energy compared to OPC-based concrete. Only LC3-0.9 showed comparable pre-peak absorbed energy to OPC-0.9. The area under the stress-strain curve from peak to ultimate stress is considered the post-crack absorbed energy in compression () [58, 59]. According to Fig. 5b, adding 0.3% RTSF to the OPC-based concrete decreased the post-peak energy absorbed. Incorporating 0.6, 0.9, and 1.2% RTSF into the OPC-based concrete increased the of the concrete. Interestingly, 1.2% RTSF significantly affected the post-crack absorbed energy in the compression of OPC concrete. In the case of LC3-based concrete, when the volume fraction of RTSF increased to 0.9% in the concrete, the post-crack energy increased sharply and then dropped when 1.2% of recycled steel fibers were added. The reduction of the in the LC3-1.2 can be attributed to the disturbance of internal homogeneity of concrete caused by the addition of a high dosage of RTSF in the LC3 concrete. The plain LC3-based concrete showed lower than plain OPC-based concrete. Similarly, using 1.2% RTSF in LC3-based concrete decreased compared to OPC-1.2. In contrast, the post-crack

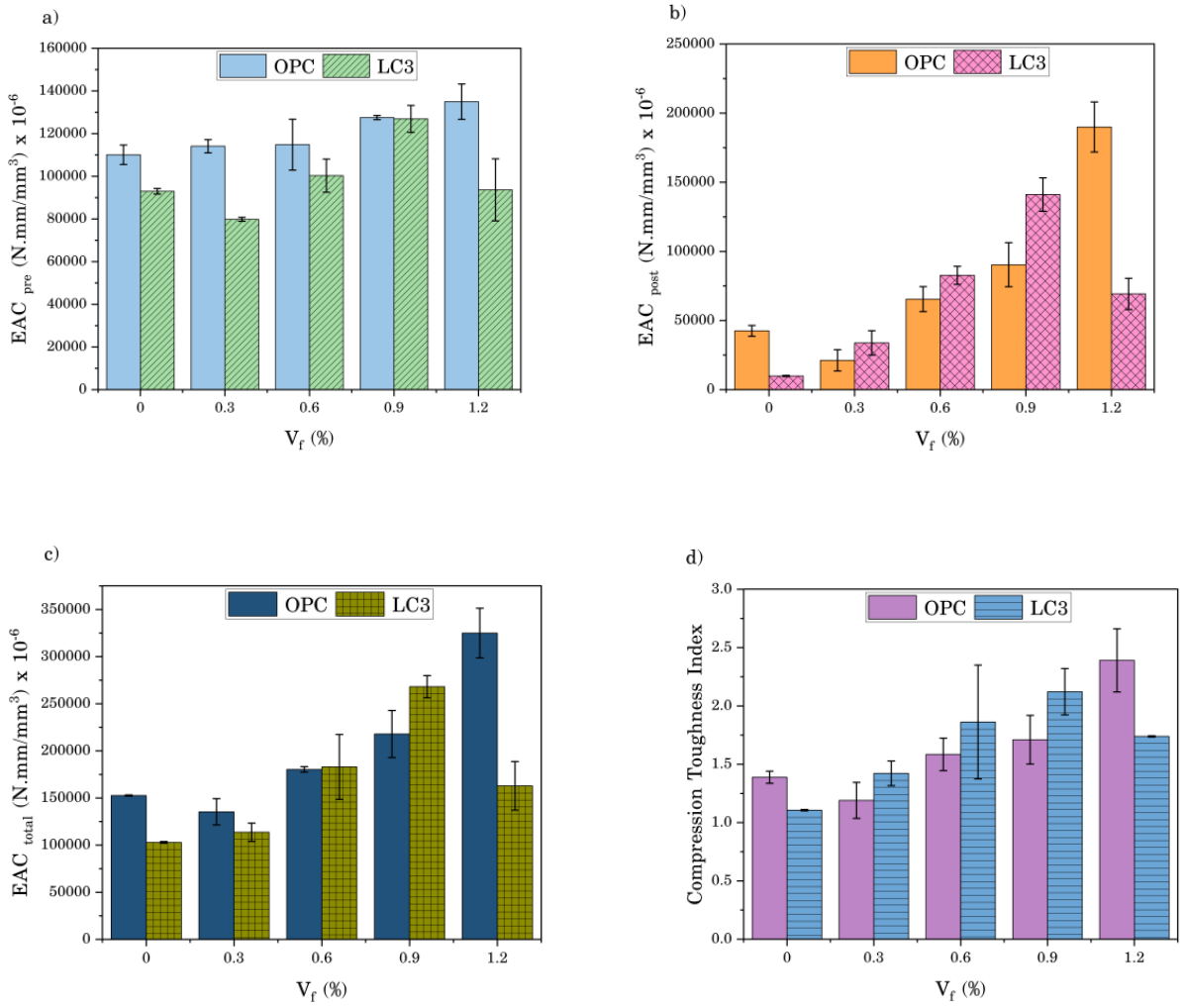

Fig. 5. a) pre-peak, b) post-peak, c) total absorbed energy in uniaxial compression, and d) compression toughness index.

energy absorbed in compression was greater in LC3-based concrete with 0.3, 0.6, and 0.9% RTSF than in OPC-based concrete with a similar amount of RTSF. Adding RTSF to concrete slightly impacted the pre-peak energy absorbed in compression. However, the beneficial effect of RTSF on the post-peak energy absorbed in compression is shown in Fig. 5b. The bridging of the cracks after peak stress by RTSF contributes to increased energy absorption. Total energy absorbed in compression () is the area under the stress-strain curve from zero to ultimate stress [58]. The results of are shown in Fig. 5c for OPC and LC3-based concrete reinforced with different amounts of RTSF. Among OPC-based concrete, only OPC-0.3 resulted in a lower amount of than plain OPC-based concrete. Adding 0.6, 0.9, and 1.2% RTSF to OPC-based concrete increased the total absorbed energy by about 18%, 43%, and 113%, respectively, compared to non-reinforced OPC-based concrete. LC3-0.9 showed the maximum amount of EAC_T among the LC3-based concrete. Adding 0.9% RTSF to the LC3-based concrete led to a 160% increase in absorbed energy compared to non-reinforced LC3. Additionally, total absorbed energy in compression increased by 10, 78, and 58% by reinforcing LC3-based concrete with 0.3%, 0.6%, and 1.2% RTSF, respectively. Only the LC3 concrete with 0.6% and 0.9% RTSF showed higher total energy absorbed in compression than the corresponding OPC-based concrete. In these cases, the post-crack absorbed energy compensated for the pre-peak energy absorbed in compression, which led to higher total absorbed energy. The toughness of concrete under uniaxial compression can be calculated by dividing the total energy absorbed by the pre-peak energy absorbed in compression (/ ()) [58]. By focusing on Fig. 5d, the compression toughness index decreased when 0.3% RTSF was added to the plain OPC-based concrete. The compression toughness index increased by including 0.6%, 0.9%, and 1.2% RTSF in the OPC-based concrete. In LC3-based concrete, the compression toughness index increased by adding RTSF up to 0.9%, and then it decreased when 1.2% RTSF was utilized. The plain and 1.2% reinforced LC3-based

concrete demonstrated a lower compression toughness index than OPC and OPC-1.2, respectively. Incorporating 0.3%, 0.6%, and 0.9% RTSF into the LC3-based concrete led to a greater compression toughness index than OPC-based concrete with the same amounts of RTSF. The secondary reactions governed by low-kaolinite calcined clay and limestone can strengthen the bonding between RTSF and the paste matrix. This positively affects the post-peak energy absorbed and compression toughness.

4- 2- Indirect Splitting Tensile

4- 2- 1- Load-Displacement Curves

Regardless of the binder system, as listed in Table 7, the splitting strength was increased by incorporating more RTSF into the concrete, which was stated in previous studies [28, 60]. The bridging action of RTSF could restrict the crack propagation and participate in load carrying, which leads to an enhancement in the splitting strength of the concrete [61]. However, the LC3-based concrete showed lower splitting strength than the OPC-based concrete when the same amount of RTSF was used. According to Table 7, the mix containing RTSF showed lower amounts of the COV compared to the plain mixes. Three main factors, including concrete mix design, quality control, and test procedure, govern the COV of the obtained results. Based on acceptable COV for compressive strength results, it can be concluded that the higher values of COV in the splitting strength test are related to the test procedure and method. The splitting tensile test is very sensitive to internal and surface defects of the concrete specimens, such as voids, cracks, and weak points. Besides, the inconsistency and irregularity of the specimen surface lead to stress concentration, which increases the COV of splitting results. However, using recycled tire steel fibers can diminish the COV of the splitting results.

The load-displacement curves of plain and recycled fiber-reinforced concrete under splitting load are shown in Figs. 6 and 7 for OPC and LC3-based concrete, respectively. OPC and LC3 concrete without fiber reinforcement broke into

Table 7. The splitting strength of the OPC and LC3-based concrete reinforced with RTSF.

Mix code	OPC	OPC-0.3	OPC-0.6	OPC-0.9	OPC-1.2
$f_{t,sp}(MPa)$	4.10	5.04	5.96	6.72	7.08
COV (%)	19.62	2.94	6.54	7.08	9.00
Mix code	LC3	LC3-0.3	LC3-0.6	LC3-0.9	LC3-1.2
$f_{t,sp}(MPa)$	3.73	4.53	5.09	5.9	6.81
COV (%)	10.92	3.91	3.89	4.29	2.46

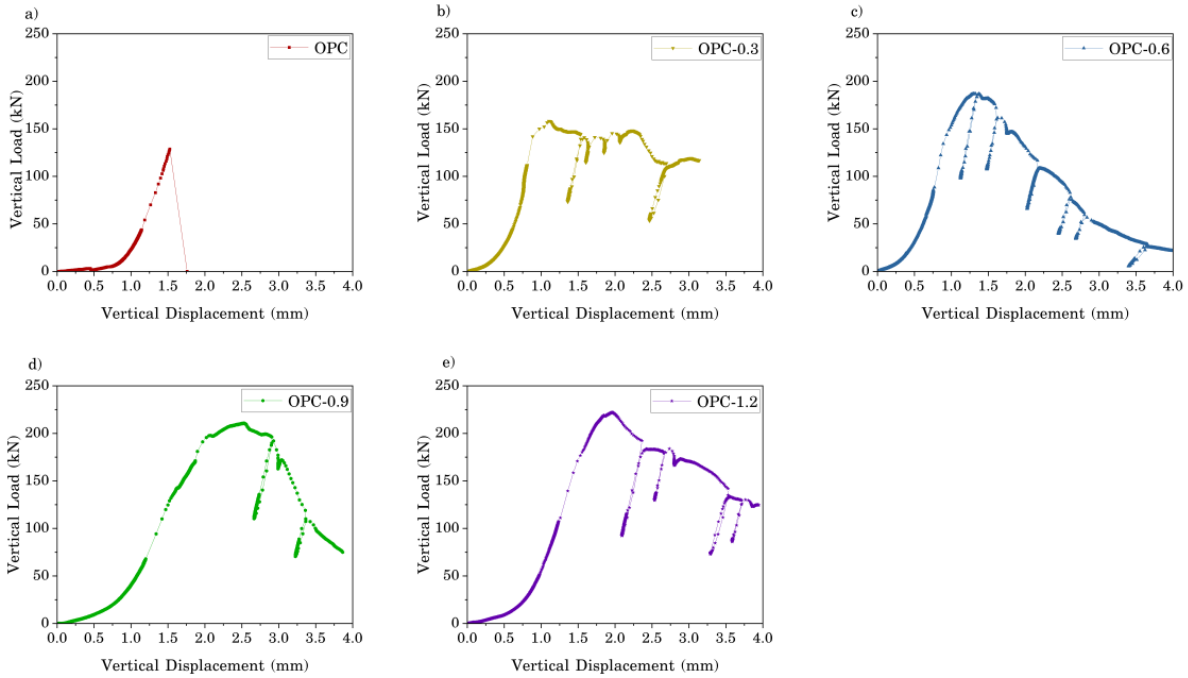

Fig. 6. The load-vertical displacement of OPC concrete under splitting tensile load.

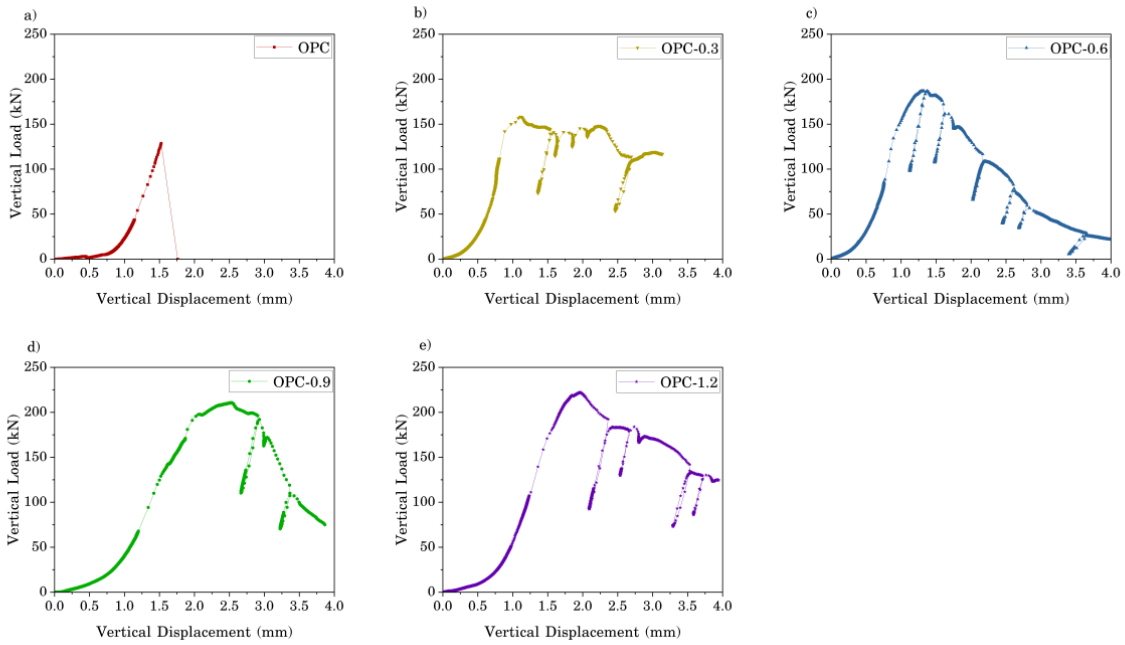

Fig. 7. The load-vertical displacement of LC3 concrete under splitting tensile load.

two specimens after the first crack occurred. As a result, the first crack and peak load of splitting are the same in the non-reinforced concrete. Reinforcing concrete with RTSF provides resistance against crack propagation, preventing the specimen from breaking into two pieces after the first crack. As a result, there is potential for the load capacity to reach peak load after the first crack in RTSF-reinforced OPC and LC3-based concrete. After peak load, OPC and LC3-based concrete reinforced with different amounts of RTSF experienced a softening part. In the softening phase of the load-displacement diagram, there are some sudden drops in load due to the failure of a group of fibers, which leads to crack propagation. This phenomenon can motivate new groups of fibers and increase the splitting load capacity close to the pre-drop load capacity. It should be noticed that OPC-0.3 and LC3-0.3 failed at the deflection of 3.14 and 2.51 mm.

4- 2- 2- Absorbed Energy and Toughness under Splitting Tensile

The area under the load displacement curve is the energy absorbed in the splitting test. Accordingly, the area under the load-displacement curve from zero to the first crack load is taken as the pre-crack energy absorbed in the splitting (). Post-crack energy absorbed in the splitting () is calculated as the area under the load displacement curve from the first crack to peak load. The area under the load-displacement curve from zero to peak load is taken as the total energy absorbed in the splitting () [58]. The results of absorbed energy, according to the load-displacement curves, are shown in Table 9 for OPC and LC3-based concrete. Incorporating 0.9% RTSF into the OPC concrete led to maximum pre-crack, post-crack, and total crack-absorbed energy in the splitting test. In LC3-based concrete, as the fiber content increased, the pre-crack absorbed energy developed. The post-crack energy absorbed had the highest amount in the LC3 concrete with 0.9% RTSF. Interestingly, in LC3-0.9, the post-crack absorbed energy compensated for the deficiency of pre-crack absorbed energy compared to LC3-1.2 and presented the maximum total energy absorbed during the splitting test. Opposite to the trend of total absorbed energy in the splitting test, the OPC and LC3-based concrete with 1.2% RTSF presented the maximum peak splitting strength and residual strength at the end. By comparing OPC and LC3-based concrete reinforced with different amounts of RTSF, it can be concluded that the OPC-based concrete presented a higher amount of pre-crack absorbed energy compared to LC3-based concrete with a similar amount of fiber. In contrast, the LC3-based concrete with RTSF demonstrated greater post-crack absorbed energy than RTSF-reinforced OPC-based concrete. Finally, the pre-crack absorbed energy surpasses the post-crack absorbed energy, resulting in a higher total absorbed energy in recycled fiber-reinforced OPC-based concrete than in similar LC3-based concrete. The splitting toughness is calculated by dividing the total absorbed energy by the pre-crack absorbed energy in the splitting test () [58]. Also, it is required to balance the splitting toughness and splitting strength. The results of splitting toughness based on load-displacement curves are represented in Table 8. Based on the load-displacement curves, OPC-0.9 exhibited the highest splitting toughness of 1.64 among OPC-based concrete. Similarly, a splitting toughness of 2.44 was calculated for LC3-0.9, which is the most significant in RTSF-reinforced LC3-based concrete. In addition, all LC3-based concrete showed higher splitting toughness than OPC-

Table 8. The absorbed energy in different stages of splitting tensile load.

	EAS_{pre}	EAS_{po}	EAS_{total}	STI		EAS_{pre}	EAS_{po}	EAS_{total}	STI
Mix code	$kN.mm$	$kN.mm$	$kN.mm$	-	Mix code	$kN.mm$	$kN.mm$	$kN.mm$	-
OPC-0.3	65.04	0	65.04	1.00	LC3-0.3	48.07	14.45	62.52	1.30
OPC-0.6	101.87	13.87	115.74	1.14	LC3-0.6	58.92	20.72	79.64	1.35
OPC-0.9	146.22	92.92	239.14	1.64	LC3-0.9	69.15	99.58	168.73	2.44
OPC-1.2	138.87	26.49	165.36	1.19	LC3-1.2	107.43	38.97	146.4	1.36

based concrete. At the initial loading level, the micro-cracks start to propagate, which can be bridged by the micro-fibers. Increasing the load leads to the micro-cracks developing into meso-cracks, which can be arrested by meso-fibers. With a further increase in the load, the meso-cracks change into the macro-cracks, which the macro-fibers can banish. As a result, the hybrid fibers, by arresting the multi-level cracks, are very effective in increasing the performance of the concrete [62]. In the removal procedure of steel fibers from expired tires, steel fibers with different lengths are produced, which can be considered hybrid steel fibers with beneficial effects on crack arresting and bridging. The hybrid action of RTSF can lead to high splitting toughness by arresting and bridging multi-level cracks in the concrete bulk, which tremendously enhances the performance of the concrete under tensile loads. A previous study by Hu et al. revealed that orientation and fiber-matrix interaction control the behavior of RTSF-reinforced concrete after crack opening [63]. Consequently, the fibers manage the behavior of fibrous concrete in the post-crack phase. LC3-based concrete reinforced with different amounts of fibers resulted in more post-crack absorbed energy and splitting toughness compared to fibrous OPC-based concrete with the same amount of RTSF. It can be concluded that the bonding strength between RTSF and the paste matrix is greater in LC3-based concrete than in OPC-based concrete. The higher bonding strength between RTSF and concrete can be related to secondary reactions governed by the mixture of limestone and low-kaolinite calcined clay, which can improve the ITZ surrounding the fibers, as proved by previous studies [57]. It was stated [57] that low-grade calcined clay can improve the particle size distribution of the mixture, enhancing the bulk density of the fiber-paste ITZ. In addition, the thermogravimetric analysis results demonstrated that low kaolinite calcined clay consumes the cement hydration products and forms C-S-H and ettringite, resulting in a denser and stronger ITZ around the fibers.

4- 3- Failure Mode Under Splitting Tensile

To determine the failure mode of RTSF-reinforced concrete under indirect splitting tensile loading, the digital image correlation (DIC) technique was employed. Initially, random black points were painted on the specimen section with a white background. Then, a high-resolution camera recorded the transformation of the section during splitting loading (see Fig. 1b). Finally, the images were extracted from high-quality video and used as the input for image processing. The image processing was conducted using the ncorr application in the MATLAB software. By analyzing these random black points, the strain in each direction of the section could be measured. The section's failure modes and lateral strain under the indirect splitting test for OPC and LC3-based concrete reinforced with different fiber volumes are presented in Figs. 9 to 16. The results of DIC are beneficial when they are linked with load-displacement curves. For example, Fig. 8 displays the load-displacement curve of LC3-based concrete reinforced with 0.9% RTSF, along with the corresponding DIC results at different stages of loading. Following this, the section's crack pattern, crack propagation, and lateral strain within the section can be coupled with the load capacity and vertical displacement under splitting tensile load.

RTSF with different lengths can bridge micro and macro cracks and prevent crack propagation. More fibers can bridge more cracks, which justifies the beneficial effects of RTSF on the crack width and propagation speed, as reported in [64]. Focusing on Figs. 9a to 12a, it can be concluded that the time of the first crack slightly changed when the fiber content increased from 0.3% to 0.6%. In contrast, the first crack time increased by adding 0.9% and 1.2% RTSF to the concrete. As a result, recycled steel fibers delay the first crack under splitting tensile, which agrees with the previous study [18]. According to the results, adding more recycled steel fibers to concrete effectively leads to narrower cracks and lesser lateral strain on the section of the specimens.

The failure mode and lateral strain of RTSF-reinforced LC3-based concrete are visible in Figs. 13 to 16. In LC3-based concrete, increasing the fiber volume to 0.9% increased the first crack time. However, the first crack time decreased when incorporating 1.2% RTSF. Also, adding 0.9% RTSF was very effective in controlling the lateral strain of the section. At 600 seconds, the lateral strain dropped when the fiber volume increased from 0.3% to 0.9%, while it increased when including 1.2% RTSF into LC3 concrete. Generally, LC3-based concrete resulted in a lower first crack time than OPC-based concrete. This can be related to the lower strength of LC3-based concrete, which leads to an earlier first crack.

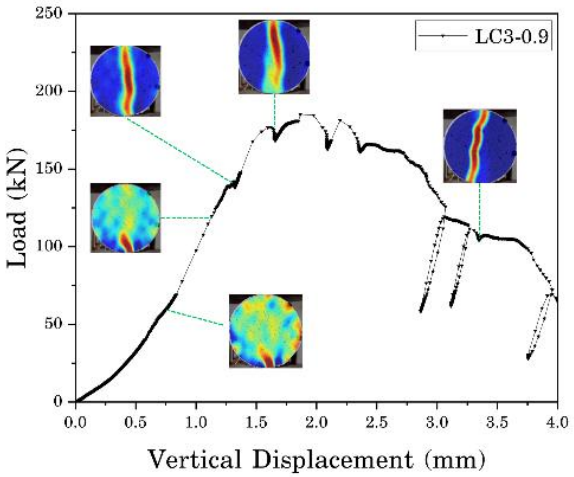

Fig. 8. The relation between DIC results and load-displacement curve under splitting tensile.

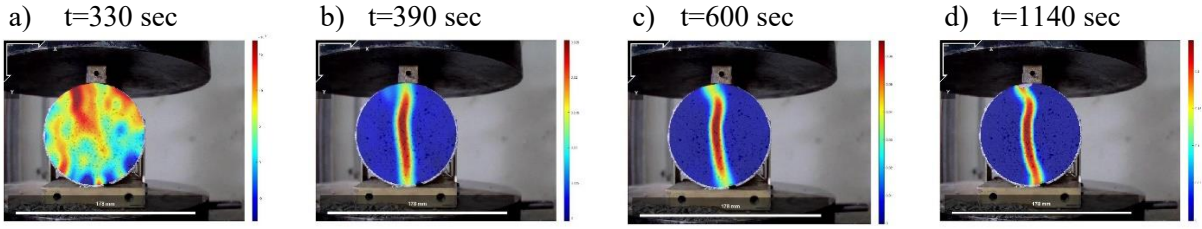

Fig. 9. The failure mode of 0.3% reinforced OPC concrete under splitting tensile load.

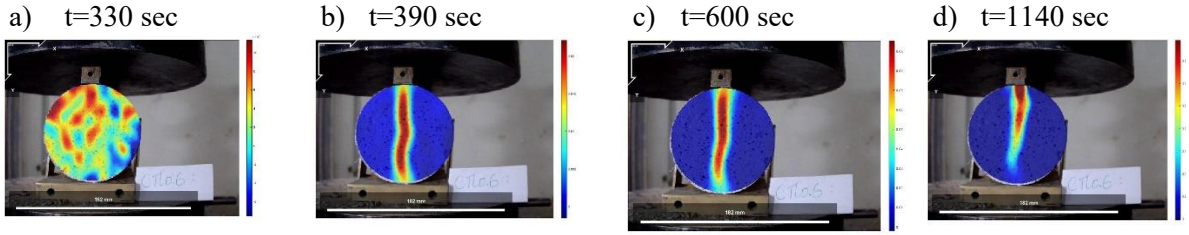

Fig. 10. The failure mode of 0.6% reinforced OPC concrete under splitting tensile load.

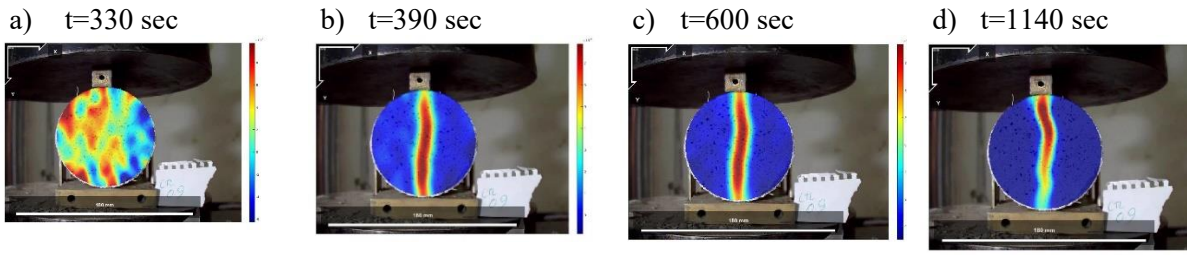

Fig. 11. The failure mode of 0.9% reinforced OPC concrete under splitting tensile load.

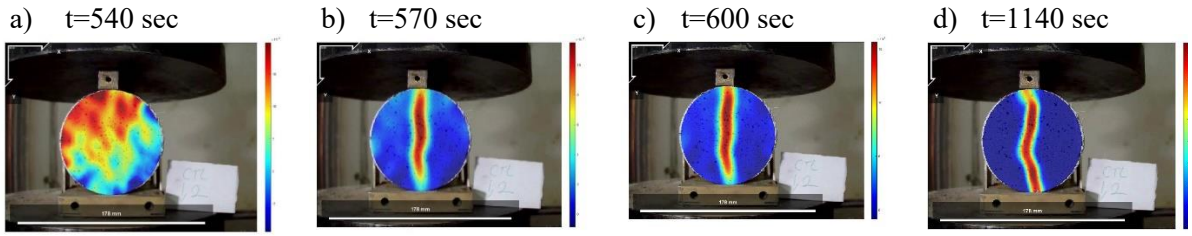

Fig. 12. The failure mode of 1.2% reinforced OPC concrete under splitting tensile load.

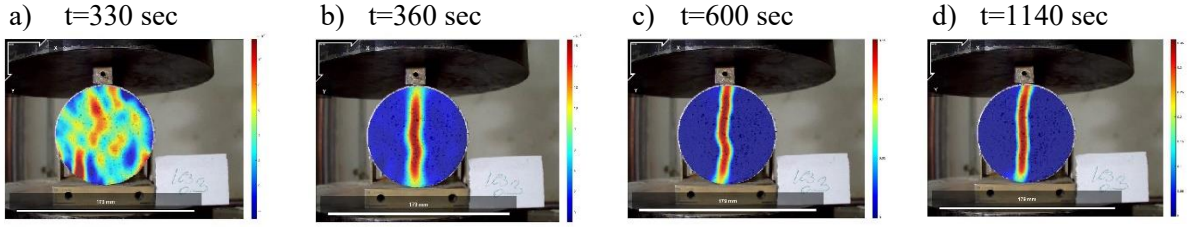

Fig. 13. The failure mode of 0.3% reinforced LC3 concrete under splitting tensile load.

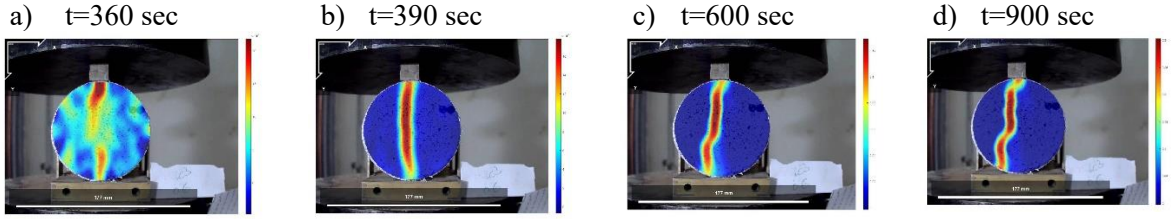

Fig. 14. The failure mode of 0.6% reinforced LC3 concrete under splitting tensile load.

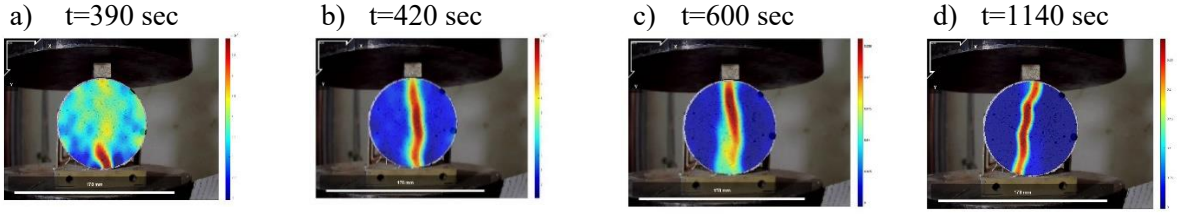

Fig. 15. The failure mode of 0.9% reinforced LC3 concrete under splitting tensile load.

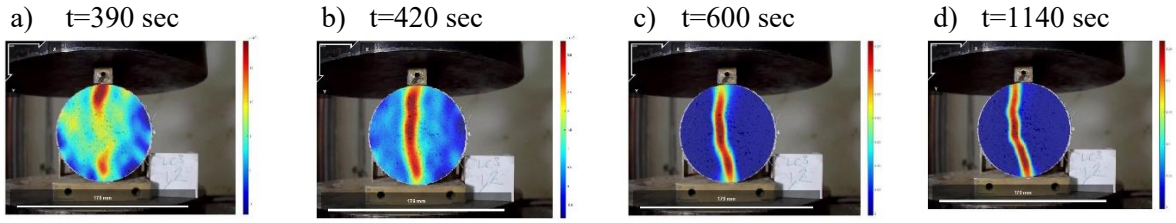

Fig. 16. The failure mode of 1.2% reinforced concrete under splitting tensile load.

5- Conclusion

In this study, high-strength OPC and LC3-based concrete were reinforced with different volume fractions of RTSF. In the LC3 concrete, 30% of the cement was substituted with the low kaolinite calcined clay and limestone mixture. To investigate the effect of RTSF on the compressive stress-strain and splitting load-deflection behavior, four volume fractions of RTSF were considered (0.3%, 0.6%, 0.9%, and 1.2%). The high-strength RTSF-reinforced OPC and LC3-based concrete were subjected to uniaxial compression and indirect splitting tensile. The following results were obtained:

Adding 0.3% RTSF to the OPC and LC3 concrete marginally changed the post-peak phase of the stress-strain curve. However, incorporating more than 0.6% RTSF into the concrete improved the compressive post-peak branch. All LC3-based concrete showed lower peak strain than the corresponding OPC-based concrete. Additionally, except for LC3 concrete reinforced with 0.9% RTSF, LC3-based concrete demonstrated less ultimate strain than OPC-based concrete.

OPC-based concrete showed higher pre-peak energy absorbed than LC3-based concrete under uniaxial compression. Only plain LC3 and LC3-1.2 demonstrated lower post-crack energy absorbed than the corresponding OPC concrete. Except for LC3-0.6 and LC3-0.9, other LC3-based concrete resulted in less total energy absorbed in compression compared to similar OPC-based concrete. The highest compression toughness was recorded for OPC and LC3 concrete reinforced with 1.2% and 0.9%, respectively.

Regardless of the binder system, adding RTSF to concrete developed the post-crack phase under an indirect splitting test, resulting in significant energy absorption and ductile failure. The maximum amount of pre-crack energy absorbed in splitting occurred when incorporating 0.9% and 1.2% RTSF into OPC and LC3-based concrete, respectively. Additionally, adding 0.9% RTSF led to the highest post-crack energy and total energy absorbed in splitting for both systems. The maximum splitting toughness was obtained by reinforcing OPC and LC3-based concrete with 0.9% RTSF. Additionally, LC3-based concrete showed a higher splitting toughness than OPC-based concrete (similar to post-crack absorbed energy in splitting), which justifies the greater fiber-paste matrix bond strength in LC3-based concrete.

Based on DIC results, incorporating more RTSF into the concrete led to a greater decrease in the lateral strain and crack propagation speed.

Among LC3-based concrete, the synergistic effect of the combination of LC3 and recycled steel fibers can be observed in the 0.9% RTSF-reinforced LC3-based concrete. As a result, incorporating 0.9% RTSF into LC3-based concrete is the optimum amount for reinforcing structural elements. LC3 concrete reinforced with 0.9% RTSF can be used in earthquake-resistant frames, industrial slabs, concrete pavements, etc., where the ductility of concrete is the main concern. Furthermore, LC3 concrete with 0.9% RTSF can be considered for the structures exposed to the impact loads.

Based on the results obtained, future research can focus on the behavior of OPC and LC3-based concrete reinforced with recycled steel fibers under cyclic uniaxial compression, and indirect splitting tensile needs to be studied. The results can be used to reinforce structural elements and finite element modeling of OPC and LC3-based concrete reinforced by different amounts of RTSF.

The Symbols used in this study

symbols	definitions	unit
f'_c	Compressive strength	MPa
v_f	Fiber volume fraction	%
ε_p	Peak strain	mm/mm
ε_{ult}	Ultimate strain	mm/mm
EAC_{pre}	Pre-peak energy absorbed in compression	kN.mm/mm^3
EAC_{po}	Post-peak energy absorbed in compression	kN.mm/mm^3
EAC_{total}	Total energy absorbed in compression	kN.mm/mm^3
$f_{t,sp}$	Splitting strength	MPa
EAS_{pre}	pre-crack energy absorbed in the splitting	kN.mm/mm^3
EAS_{po}	post-crack energy absorbed in the splitting	kN.mm/mm^3
EAS_{total}	Total energy absorbed in the splitting	kN.mm/mm^3
STI	Splitting toughness index	-

References

[1] S. Mansouri, A. Rahai, S.H. Rashedi, F. Moghadas Nejad, Predicting Concrete Carbonation Depth and investigating the influencing factors through machine learning approaches and optimization, Amirkabir Journal of Civil Engineering, 56(12) (2025) 1583-1604.

[2] A. Ramezanian Pour, S. Sedighi, M. Kazemian, A. Ramezanianpour, Effect of micro silica and slag on the durability properties of mortars against accelerated carbonation and chloride ions attack. AUT J Civil Eng. 2020; 4 (4): 411–22, in.

[3] S.H. Rashedi, A. Rahai, Experimental and numerical advances in seismic assessment of continuous RC rigid-frame bridges: A review, Results in Engineering, (2025) 105656.

[4] M. Ghanbari, Environmental impact assessment of building materials using life cycle assessment, J. Arch. Environ. Struct. Eng. Res, 6 (2023) 11-22.

[5] R.-S. Lin, H.-S. Lee, Y. Han, X.-Y. Wang, Experimental studies on hydration–strength–durability of limestone-cement-calcined Hwangtoh clay ternary composite, Construction and Building Materials, 269 (2021) 121290.

[6] S. Krishnan, A.C. Emmanuel, S. Bishnoi, Hydration and phase assemblage of ternary cements with calcined clay and limestone, Construction and Building Materials, 222 (2019) 64-72.

[7] K. Scrivener, F. Martirena, S. Bishnoi, S. Maity, Calcined clay limestone cements (LC3), Cement and concrete research, 114 (2018) 49-56.

[8] S.S. Berriel, A. Favier, E.R. Domínguez, I.S. Machado, U. Heierli, K. Scrivener, F.M. Hernández, G. Habert, Assessing the environmental and economic potential of Limestone Calcined Clay Cement in Cuba, Journal of Cleaner Production, 124 (2016) 361-369.

[9] S. Sedighi, A. Rahai, F. Moodi, Multi-criteria optimization for sustainable concrete mix considering the synergistic effect of recycled steel fiber and LC3 concrete, Results in Engineering, (2025) 107809.

[10] Y. Dhandapani, M. Santhanam, Assessment of pore structure evolution in the limestone calcined clay cementitious system and its implications for performance, Cement and Concrete Composites, 84 (2017) 36-47.

[11] M. Shekarchi, A. Bonakdar, M. Bakhshi, A. Mirdamadi, B. Mobasher, Transport properties in metakaolin blended concrete, Construction and Building Materials, 24(11) (2010) 2217-2223.

[12] R. Bucher, M. Cyr, G. Escadeillas, Performance-based evaluation of flash-metakaolin as cement replacement in marine structures–Case of chloride migration and corrosion, Construction and Building Materials, 267 (2021) 120926.

[13] R.G. Pillai, R. Gettu, M. Santhanam, S. Rengaraju, Y. Dhandapani, S. Rathnarajan, A.S. Basavaraj, Service life and life cycle assessment of reinforced concrete systems with limestone calcined clay cement (LC3), Cement and Concrete Research, 118 (2019) 111-119.

[14] A. Zolfagharnasab, A.A. Ramezanianpour, F. Bahman-Zadeh, Investigating the potential of low-grade calcined clays to produce durable LC3 binders against chloride ions attack, Construction and Building Materials, 303 (2021) 124541.

[15] C. Rodriguez, J.I. Tobon, Influence of calcined clay/limestone, sulfate and clinker proportions on cement performance, Construction and Building Materials, 251 (2020) 119050.

[16] G. Argın, B. Uzal, Enhancement of pozzolanic activity of calcined clays by limestone powder addition, Construction and Building Materials, 284 (2021) 122789.

[17] E. Rahimi, J. Shafaei, M. Esfahani, Experimental Evaluation of Structural Performance of FRC Beams with Hooked Metal and Macro Polymer Fibers at Different Levels of Reinforcement Corrosion, Amirkabir Journal of Civil Engineering, 53(4) (2021) 1275-1294.

[18] T.A. Mehmandari, M. Shokouhian, M. Imani, K. Tee, A. Fahimifar, Split Tensile Behavior of Recycled Steel Fiber-Reinforced Concrete, ACI Materials Journal, 122(2) (2025).

[19] T.A. Mehmandari, M. Shokouhian, M. Imani, A. Fahimifar, Experimental and numerical analysis of tunnel primary support using recycled and hybrid fiber reinforced shotcrete, in: Structures, Elsevier, 2024, pp. 106282.

[20] J. Chang, K. Cui, Y. Zhang, Effect of hybrid steel fibers on the mechanical performances and microstructure of sulphoaluminate cement-based reactive powder concrete, Construction and Building Materials, 261 (2020) 120502.

[21] T.A. Mehmandari, M. Shokouhian, M.Z. Josheghan, S.A. Mirjafari, A. Fahimifar, D.J. Armaghani, K.F. Tee, Flexural properties of fiber-reinforced concrete using hybrid recycled steel fibers and manufactured steel fibers, Journal of Building Engineering, 98 (2024) 111069.

[22] M.A. Aiello, F. Leuzzi, G. Centonze, A. Maffezzoli, Use of steel fibres recovered from waste tyres as reinforcement in concrete: Pull-out behaviour, compressive and flexural strength, Waste management, 29(6) (2009) 1960-1970.

[23] H. Hu, P. Papastergiou, H. Angelakopoulos, M. Guadagnini, K. Pilakoutas, Mechanical properties of SFRC using blended recycled tyre steel cords (RTSC) and recycled tyre steel fibres (RTSF), Construction and Building Materials, 187 (2018) 553-564.

[24] J. Krolo, D. Damjanovic, I. Duvnjak, D. Bjegovic, S. Lakusic, A. Baricevic, Innovative low-cost fibre-reinforced concrete. Part II: Fracture toughness and impact strength, Concrete Repair, Rehabilitation and Retrofitting III, CRC Press/Balkema, (2012) 204-209.

[25] K. Aghaee, M.A. Yazdi, K.D. Tsavdaridis, Investigation into the mechanical properties of structural lightweight concrete reinforced with waste steel wires, Magazine of

Concrete Research, 67(4) (2015) 197-205.

[26] H. Bensaci, B. Menadi, S. Kenai, Comparison of some fresh and hardened properties of self-consolidating concrete composites containing rubber and steel fibers recovered from waste tires, Nano Hybrids and Composites, 24 (2019) 8-13.

[27] M. Leone, G. Centonze, D. Colonna, F. Micelli, M. Aiello, Fiber-reinforced concrete with low content of recycled steel fiber: Shear behaviour, Construction and Building Materials, 161 (2018) 141-155.

[28] G. Peng, J. Yang, Q. Long, X. Niu, Y. Shi, Mechanical properties and explosive spalling behavior of the recycled steel fiber reinforced ultra-high-performance concrete, in: Multi-Span Large Bridges—Proceedings of the International Conference on Multi-Span Large Bridges, 2015, pp. 1019-1026.

[29] M.H. Sotoudeh, M. Jalal, Effects of waste steel fibers on strength and stress-strain behavior of concrete incorporating silica nanopowder, Indian Journal of Science and Technology, 6(11) (2013) 5411-5417.

[30] G. Centonze, M. Leone, E. Vasanelli, M.A. Aiello, Interface analysis between steel bars and recycled steel fiber reinforced concrete, in: Proceedings of the Fracture Mechanics of Concrete and Concrete Structures, JGM van Mier, G. Ruiz, C. Andrade, RC Yu and XX Zhang, 2013, pp. 431-441.

[31] O.D. Atoyebi, S.O., Odeyemi, S.A., Bello, C.O., Ogbeifun, Splitting tensile strength assessment of lightweight foamed concrete reinforced with waste tyre steel fibres, International Journal of Civil Engineering and Technology (IJCIET), 9(9) (2018) 1129-1137.

[32] A.H. Farhan, A.R. Dawson, N.H. Thom, Recycled hybrid fiber-reinforced & cement-stabilized pavement mixtures: Tensile properties and cracking characterization, Construction and Building Materials, 179 (2018) 488-499.

[33] S. Sarabi, H. Bakhshi, H. Sarkardeh, H.S. Nikoo, Thermal stress control using waste steel fibers in massive concretes, The European Physical Journal Plus, 132 (2017) 1-8.

[34] M.A. Köroğlu, Behavior of composite self-compacting concrete (SCC) reinforced with steel wires from waste tires, Revista de la Construcción, 17(3) (2019) 484-498.

[35] M. Jomaa'h, A. Khazaal, S. Ahmed, Effect of replacing the main reinforcement by steel fibers on flexural behavior of one-way concrete slabs, in: MATEC Web of Conferences, EDP Sciences, 2018, pp. 04010.

[36] A. ASTM, C33/c33m-18 standard specification for concrete aggregates, ASTM International: West Conshohocken, PA, USA, (2018).

[37] C. Astm, Standard test method for relative density (specific gravity) and absorption of fine aggregate, ASTM Current Edition Approved Jan, 1 (2015).

[38] C. ASTM, C127 Standard Test Method for Relative Density (Specific-Gravity) and 38 absorption of coarse aggregate, West: American Society for Testing and Materials, (2015).

[39] C. Astm, 143; Standard Test Method for Slump of Hydraulic-Cement Concrete, ASTM International, (2003).

[40] G. Centonze, M. Leone, M.A. Aiello, Steel fibers from waste tires as reinforcement in concrete: A mechanical characterization, Construction and Building Materials, 36 (2012) 46-57.

[41] G. Centonze, M. Leone, F. Micelli, D. Colonna, M.A. Aiello, Concrete reinforced with recycled steel fibers from end-of-life tires: Mix-design and application, Key Engineering Materials, 711 (2016) 224-231.

[42] K. Liew, A. Akbar, The recent progress of recycled steel fiber reinforced concrete, Construction and Building Materials, 232 (2020) 117232.

[43] H. Du, S. Dai Pang, High-performance concrete incorporating calcined kaolin clay and limestone as cement substitute, Construction and Building Materials, 264 (2020) 120152.

[44] A.I.C.C.o. Concrete, C. Aggregates, Standard test method for compressive strength of cylindrical concrete specimens, ASTM International, 2014.

[45] A. ASTM, C496/C496M-17 Standard test method for splitting tensile strength of cylindrical concrete specimens, in: American Society for Testing and Materials, 2017.

[46] Ł. Skarżyński, J. Suchorzewski, Mechanical and fracture properties of concrete reinforced with recycled and industrial steel fibers using Digital Image Correlation technique and X-ray micro computed tomography, Construction and Building Materials, 183 (2018) 283-299.

[47] S.A. Rossli, I.S. Ibrahim, Mechanical properties of recycled steel tire fibres in concrete, Fac. Civil Eng., University of Technology, (2012).

[48] P. Sharmila, G. Dhinakaran, Compressive strength, porosity and sorptivity of ultra fine slag based high strength concrete, Construction and Building Materials, 120 (2016) 48-53.

[49] L. Sun, Q. Hao, J. Zhao, D. Wu, F. Yang, Stress-strain behavior of hybrid steel-PVA fiber reinforced cementitious composites under uniaxial compression, Construction and Building Materials, 188 (2018) 349-360.

[50] E.B. Pereira, G. Fischer, J.A. Barros, Effect of hybrid fiber reinforcement on the cracking process in fiber reinforced cementitious composites, Cement and Concrete Composites, 34(10) (2012) 1114-1123.

[51] J. Shafaei, R. Eskandari, Direct Design Method for RC Columns and Uniformly Reinforced Shear Walls based on Canadian Standards, AUT Journal of Civil Engineering, 6(2) (2022) 159-174.

[52] J. Shafaei, R. Eskandari, Proposing Formula-Based Design Method for RC Columns and Uniformly Reinforced Shear Walls, AUT Journal of Civil Engineering, 4(2) (2020) 249-264.

[53] D.J. Carreira, K.-H. Chu, Stress-strain relationship for plain concrete in compression, in: Journal proceedings, 1985, pp. 797-804.

[54] A.C. 318, Building Code Requirements for Structural Concrete (ACI 318-19): An ACI Standard; Commentary on Building Code Requirements for Structural Concrete (ACI 318R-19), American Concrete Institute, 2019.

[55] M. Abu-Saleem, Y. Zhuge, R. Hassanli, M. Ellis, M.M. Rahman, P. Levett, Stress-strain behaviour and mechanical strengths of concrete incorporating mixed recycled plastics, Journal of Composites Science, 5(6) (2021) 146.

[56] G. Ren, H. Wu, Q. Fang, J. Liu, Effects of steel fiber content and type on static mechanical properties of UHPCC, Construction and Building Materials, 163 (2018) 826-839.

[57] W. Chen, J. Dang, H. Du, Using low-grade calcined clay to develop low-carbon and lightweight strain-hardening cement composites, Journal of Building Engineering, 58 (2022) 105023.

[58] M. Khan, M. Cao, M. Ali, Effect of basalt fibers on mechanical properties of calcium carbonate whisker-steel fiber reinforced concrete, Construction and Building Materials, 192 (2018) 742-753.

[59] M. Usman, S.H. Farooq, M. Umair, A. Hanif, Axial compressive behavior of confined steel fiber reinforced high strength concrete, Construction and Building Materials, 230 (2020) 117043.

[60] M. Mastali, A. Dalvand, A. Sattarifard, Z. Abdollahnejad, B. Nematollahi, J. Sanjayan, M. Illikainen, A comparison of the effects of pozzolanic binders on the hardened-state properties of high-strength cementitious composites reinforced with waste tire fibers, Composites Part B: Engineering, 162 (2019) 134-153.

[61] M. Mastali, A. Dalvand, A. Sattarifard, Z. Abdollahnejad, M. Illikainen, Characterization and optimization of hardened properties of self-consolidating concrete incorporating recycled steel, industrial steel, polypropylene and hybrid fibers, Composites Part B: Engineering, 151 (2018) 186-200.

[62] C. Ostertag, J. Blunt, Effect of crack control in hybrid fiber reinforced concrete composites on corrosion rate of steel reinforcing bars, Seoul: Korea Concrete Institute, (2010).

[63] H. Hu, P. Papastergiou, H. Angelakopoulos, M. Guadagnini, K. Pilakoutas, Mechanical properties of SFRC using blended manufactured and recycled tyre steel fibres, Construction and Building Materials, 163 (2018) 376-389.

[64] K.B. Najim, A. Saeb, Z. Al-Azzawi, Structural behaviour and fracture energy of recycled steel fibre self-compacting reinforced concrete beams, Journal of Building Engineering, 17 (2018) 174-182.

HOW TO CITE THIS ARTICLE

S. Sedighi, A. R. Rahai, F. Moodi, The Behavior of High-Strength LC3 Concrete Reinforced with Recycled Steel Fiber under Uniaxial Compression and Splitting Tensile, AUT J. Civil Eng., 9(4) (2025) 337-356.

DOI: 10.22060/ajce.2025.24264.5927